Article

Successive Optimization of a Homogeneous Immunoassay for Antibody Detection in Viral Infections

Lina S. Franco [1,*], Vladimiro Mujica [1], Joseph N. Blattman [2] and Antonio A. Garcia [3]

[1] School of Molecular Sciences, Arizona State University, Tempe, Arizona, U.S.A.; lsfranco@asu.edu, vmujica@asu.edu
[2] School of Life Sciences, Arizona State University, Tempe, Arizona, U.S.A.; joseph.blattman@asu.edu
[3] School of Biological and Health Systems Engineering, Arizona State University, Tempe, Arizona, U.S.A.; tony.garcia@asu.edu
* Correspondence: lsfranco@asu.edu; Tel.: +1-480-965-4295

Abstract: Although there are extensive literature reports on the use of gold nanoparticle (AuNP) based homogeneous assays for detection of biomolecules, very few experimental description and procedures involving their preparation are described. In this study, AuNPs conjugated to Bovine Serum Albumin or Envelope protein from Dengue II were developed as a homogeneous immunoassay for antibody detection. We report here optimization of key parameters to prepare an immunoassay like conjugation protein concentration, centrifugation time, electrolyte addition and assay temperature. We determined that saturating protein concentrations improved AuNPs surface coverage and uniformity of the assay and addition of sodium chloride improved sensitivity of the antibody detection method and assay stability. Furthermore, we showed that dynamic light scattering can be used to monitor changes in gold nanoparticles in the preparation and detection steps. Additionally, numerical simulations of the plasmonic optical response of AuNPs were carried out to scan for size-dependent response of the AuNPs. The AuNPs homogeneous immunoassay developed was further used in the detection of antibodies *in vitro* to detect Dengue virus infection.

Keywords: gold nanoparticles; homogeneous immunoassay; antibody detection; virus infection; Dengue Protein E.

1. Introduction

Homogeneous assays, in which the sample is analyzed in the liquid phase and requires no further separation steps, have been developed as a means to increase assay responsiveness and/or analysis speed, as well as improve sensitivity by utilizing instrumentation suitable for liquid phase measurement. Over the past 25 years, one of the most significant developed homogeneous assays utilizes AuNPs for the detection of molecules in plasma or other biomarkers because of its surface plasmonic properties [1-4]. However, important challenges remain when translating their use for sensitive homogeneous assays [5,6]. The lack of detailed descriptions of the construction steps of the AuNP based assay can lead to confusion regarding optimal preparation and low sensitivity or spurious results may occur.

In the procedure to develop a homogeneous immunoassay using AuNPs, three main parts have been identified: *i)* the conjugation of the protein to AuNPs, *ii)* purification of conjugated AuNPs via centrifugation and *iii)* incubation with sample to be detected. Previously, it has been proposed that the grafting of the protein on the surface of AuNPs occurs either through near-covalent gold-thiol bonds (directional) or non-covalent bonding (electrostatic) [7-9]. In the case of electrostatic binding, the amount of protein needed to cover the surface of the AuNPs is usually determined by titration of

Preprints (www.preprints.org) | NOT PEER-REVIEWED | Posted: 21 August 2018 doi:10.20944/preprints201808.0370.v1

the coating protein. However, the titration is not always efficient determining the coverage of all the nanoparticles, but only the majority of them, and can result in increased non-specific binding of analyte and less efficiency [10]. The purification step based on the optimization of the centrifugation parameters is critical to remove free protein in solution to avoid unspecific binding of free protein to conjugate with their target [11]. Speed and times in this step vary depending on the size of the AuNPs, but resuspension of the functionalized AuNPs to have a colloidal stable dispersion is not well described in literature. Finally, incubation of the AuNPs with the sample has been described at varying temperatures, but have not been accurately assessed for variance.

In the work presented herein, we have addressed the preparation of a homogeneous immunoassay for detection of viral infections using AuNPs, followed by the evaluation of its efficiency and monitoring of its colloidal stability during use. We describe the results obtained for the development of two specific homogeneous assays for detection of anti-BSA and anti-Protein E antibodies using AuNPs of 60 nm nominal diameter conjugated with BSA and recombinant Dengue virus (DENV-2) Protein E, respectively. Specifically, we optimize these processes using different concentrations of protein during gold nanoparticle conjugation, centrifugation conditions to remove unbound protein, the addition of electrolytes to increase sensitivity, and finally the importance of incubation temperature on the stability of AuNPs and assay results. Results of light extinction and light scattering are further confirmed with ELISA for the system described. Furthermore, computational studies based on Mie Theory of the plasmonic response of AuNPs were carried out that validated the consistency of our results. This study provides researchers interested in the development of nano-biosensors for the detection of antibodies with a thorough analysis for the use of AuNPs in homogeneous immunoassays for detection of past and current viral infections.

2. Materials and Methods

Buffers, Solutions and Antibodies

Phosphate Buffered Saline (PBS) with 0.2% sodium azide, 1 M acetate buffer (pH = 5), 1 M borate buffer (pH = 8.5), and sodium chloride (5 M) were prepared. Bovine Serum Albumin (Boston Bioproducts, Ashford, MA https://bostonbioproducts.com) was dissolved in freshly prepared pH = 5 acetate buffer (Fisher Scientific, Pittsburgh, PA https://www.fishersci.com/) to create a stock solution of 10 mg/ml BSA. Recombinant DENV-2 Envelope Protein 32 kDa produced in *E. coli* (Reagent Proteins, San Diego, CA http://www.reagentproteins.com) was purchased with a concentration of 0.96 mg/ml. Polyclonal anti-BSA antibody from rabbit (Rockland Immunochemicals, Lemerick, PA https://www.rockland-inc.com/), polyclonal anti-Envelope protein antibody from goat (1 mg/ml), and lyophilized human serum (Rockland Immunochemicals, Lemerick, PA https://www.rockland-inc.com/) were diluted with PBS containing azide. The monoclonal anti-GP1 antibody (0.2 mg/ml; Acris antibodies, Rockville, MD https://www.acris-antibodies.com) used in the experiments reacts with Lymphocytic Choriomeningitis virus (LCMV) from infected mouse cells.

Conjugation of AuNPs to BSA or Protein E

For BSA conjugation, in a 1.5 ml eppendorf tube an aliquot of 1 ml containing 2.6 x 10^{10} particles/ml of 60 nm citrate stabilized spherical gold colloids (AuNPs) (Ted Pella Inc, Redding, CA, http://www.tedpella.com) were combined with 10 µl of 1 M acetate buffer pH = 5 prior to the addition of 100 µl of 0.1 - 10 mg/ml BSA. For protein E conjugation, 100 µl of 1 M borate buffer and 4-50 µl of 0.85 mg/ml of recombinant DENV-2 protein E were added to 1 ml of 60 nm AuNPs. The mixture was gently rocked at 4 ˚C using an orbital table for 30 minutes.

After incubation, 2.5 µl of a 10% solution of Tween 20 (Sigma-Aldrich Corp., St. Louis, MO http://www.sigmaaldrich.com) was added to the mixture rocking for 5 min. Three centrifugation steps were conducted to reduce the concentration of free BSA in solution. The conditions were adapted from Cytodiagnostics Inc. (www.cytodiagnostics.com). A Beckman Coultor Microfuge 18 was placed in at 4 ˚C. The first centrifugation was for 30 minutes at 1125×*g* or 3350 rpm. Immediately after centrifugation, the supernatant was carefully removed. Then, 1 ml of the buffer

 doi:10.20944/preprints201808.0370.v1

initially used for each protein was added to re-suspend the pellet. 2.5 µl of 10% Tween 20 was added to the suspension and the mixture was rocked for 5 minutes. Afterwards, the suspension was centrifuged for 15 minutes at 3350 rpm and the supernatant was removed carefully. For the third centrifugation, time was shortened to 10 minutes at 3350 rpm. After the third centrifugation, the pellet was re-suspended in 1 ml PBS buffer with azide when BSA was conjugated, and 0.5 ml of 0.2 mg/ml BSA was used as a blocking agent along with 0.5 ml of PBS, in the case of Protein E conjugation. Stoichiometric calculations to determine the amount of protein of the surface of the gold nanoparticles were calculated using the surface area of the AuNPs and the estimated surface coverage of the protein (BSA or protein E).

Detection of anti-BSA or anti-Protein E antibodies using AuNPs based Homogeneous Immunoassay

For detection of anti-BSA antibody, aliquots of 100 µl of BSA conjugated to AuNPs (BSA-AuNPs) solution were diluted with 900 µl of PBS and aliquots of 10 µl of different concentrations of anti-BSA antibody diluted in PBS (0-10 µg/ml) were added. To determine the most suitable incubation temperature, the BSA-AuNPs were mixed with different concentrations of anti-BSA antibody and incubated for 0 or 30 min at two different temperatures (20 ˚C or 37 ˚C). Changes in size and optical properties were determined for 3-5 replicates using static and dynamic light scattering.

For detection of anti-protein E antibody both in buffer and in reconstituted human serum, experiments for performed similarly as with the BSA-AuNPs with some modifications. Incubation with the antibody was performed at 37 ˚C for 30 min and static light scattering measurements were performed for 3-5 replicates of each sample immediately after incubation.

Detection of anti-BSA antibody using ELISA

The assay was performed as recommended by Sigma-Aldrich with some modifications [12]. Wells of polystyrene microtiter plates were coated for 2 h at room temperature with different BSA solutions: 5 µg/ml BSA/0.25% of Tween 20, 5 µg/ml BSA/0.5 M NaCl, 10, 5, 1 and 0 µg/ml in 0.1 M sodium carbonate-bicarbonate buffer (pH = 9.6). Optical density was read at 490 nm and compared to two negative controls: uncoated wells and an anti-GP1 antibody specific for lymphocytic choriomeningitis virus (LCMV).

UV/Vis Spectroscopy and Light Scattering measurements

An Ocean Optics Fiber Optic Spectrometer (Ocean Optics, Dunedin, FL, http://oceanoptics.com) was used for UV/Vis spectra acquisition using a USB4000 spectrometer and SpectraSuite Software for control and data acquisition. A quartz cuvette of 1 cm path length was used to acquire samples. Two different light sources were employed for measurements: for UV detection and standard Vis spectroscopy, a Deuterium Halogen light source, and for higher resolution visible spectroscopy, a 12 W 350 mA (Titanium) LED source. Spectra for UV/Vis data was generally collected between 10-100 milliseconds integration time and 20-100 spectra were averaged for each sample, depending upon the light source. The drift in spectral recordings was negligible.

For static light scattering measurements, a InPhotonics 532 nm laser with an Ocean Optics controller was used in a 90° configuration from the fiber optic collector to measure counts. Readings over 1 second of integration and only 2 spectra were used for averaging.

For dynamic light scattering measurements, a Beckman Coulter DelsaNano C particle analyzer was used to perform size analysis (with 50 measurements over 2 secs for each sample) with CONTIN, Marquandt or NNLS analysis to obtain the intensity distribution.

Mie theory-based numerical simulations

All Mie theory calculations for light extinction and light scattering were made with the Mie theory calculator from nanoComposix website (http://nanocomposix.com/pages/tools).

Preprints (www.preprints.org) | NOT PEER-REVIEWED | Posted: 21 August 2018 doi:10.20944/preprints201808.0370.v1

3. Results

3.1. Light scattering detection of AuNPs and theoretical comparison

To predict light extinction of the different systems to be studied, the Rayleigh approximation of the Mie theory for light scattering of smaller particles and the Guinier approximation for larger particles were used using the concentration provided by the manufacturer and the total surface area of AuNPs. [13-15]. These results were compared with the experimental data collected from using citrate capped AuNPs as a function of the size. The raw data collected by the spectrometer and the online Mie Theory calculator values exhibit a good agreement (Figure 1): both computational and experimental results show the extinction maxima shift to higher wavelengths and increasing in intensity. Also, the three largest sized nanoparticles (100 and 200 nm) do not have extinction curves that approach zero at 750 nm. These similarities are relevant to subsequent use of light extinction to interpret immunoassay test results have been identified.

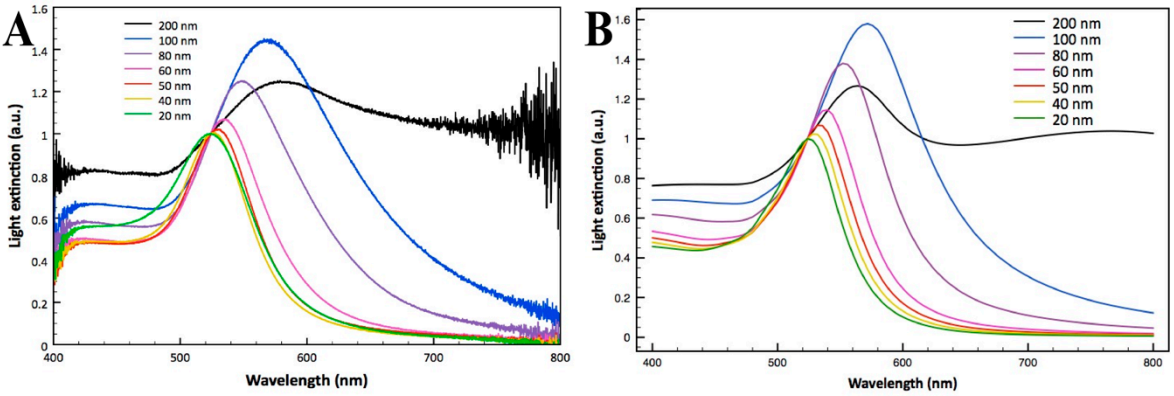

Figure 1. Predicted and experimental light extinction from gold nanoparticles of different sizes. Extinction measurement of gold nanoparticles with equal gold concentration, but size varying as shown: 20, 40, 50, 60, 80, 100 and 200 nm. (**a**) Measured using a visible light spectrometer and (**b**) from calculations from the Nanocomposix web site.

For static light scattering, a basis of comparison between the theoretical calculations and the 532 nm green laser 90° light scattering used experimentally is not straight-forward, due to the manner used in collecting scattering and recording counts. To interpret the theoretical predictions, it is required to introduce limits based on scattering regimes that predominate in particles ranging from 20 – 200 nm in diameter (Figure S1). The main graph shows the relative scattering intensity as a function of the AuNP diameter. The inset shows the Online Mie Scattering extinction (contribution of scattering to the absorbance measured) due to scattering at 532 nm versus the experimentally measured scattering counts. As expected, there is a linear correlation between these. For the purpose of comparison and interpretation, the correlation shown in the inset is useful for predicting the expected increase in static light scattering measured with small aggregates.

3.2. Conjugation of BSA and DENV-2 Protein E to AuNPs

After comparing results with the theoretical predictions, we stablished we could use light scattering and light extinction to measure unconjugated gold nanoparticles of different sizes. For conjugation, the pH of the buffer used to attach the proteins to the surface of the AuNPs stablishes the net charge of the protein and as consequence affects the protein-surface interactions. Acetate buffer (pH = 5) was used to asses that the majority of the protein species (BSA) is neutral. To determine the amount of buffer necessary to add to 1 ml of AuNPs, different amounts of acetate buffer were tested (10 µl to 100 µl). Adding more than 50 µl of acetate buffer induced aggregation of the AuNPs, evidenced by a color change in the solution, from pink to purple or gray, and the

 doi:10.20944/preprints201808.0370.v1

appearance of tailing in the 600-800 nm region in the visible light extinction spectrum. The absence of the tailing when the AuNPs are dispersed in the presence of 10 µl of acetate buffer confirms the colloidal stability of the AuNPs in the conjugation medium (not shown).

The amount of protein (conjugate) required to cover the surface of the AuNPs, prevent aggregation and provide colloidal stability of the protein surface modified AuNPs in the presence of sodium was first approached by stoichiometric calculations. For the conjugation of BSA to the surface of the AuNPs, an average of 10 molecules of BSA was calculated to achieve the required conditions, hence, a concentration of 0.5 mg/ml of BSA was used. The conjugation was achieved by incubation of the protein with the AuNPs rocking the mix for 30 minutes at room temperature with an ice pack. This was confirmed visually after final re-suspension with PBS by a lack of color change. Alternatively, Tsai *et al* (2011) referred that to get a 90% coverage of the gold nanoparticle of the same size, at least a 2 mg/ml BSA solution was needed. For this reason, a 7 mg/ml solution of BSA in DI H_2O was also used for the conjugation step to ensure the maximal saturating coverage of the gold nanoparticles. The procedure was repeated resulting in a lack in color change of the gold nanoparticles in the presence of PBS, and the visible spectrum showed no signs of aggregation compared to the spectrum of the gold nanoparticle solution before conjugation (not shown).

In the case of the conjugation of DENV-2 protein E peptide to the surface of AuNPs a borate buffer (pH = 8.5) was chosen. Three different amounts of protein E (8.5, 17 and 42.5 µg) were added to 1 ml of 60 nm AuNPs, showing that 42.5 µg was a sufficient amount of protein to cover the gold nanoparticles and prevent the aggregation in the presence of PBS after the last re-suspension. The dispersion was stable for more than 2 hours.

3.3. Centrifugation of conjugated AuNPs

The removal of the non-conjugated protein species was achieved by a centrifugation procedure. The importance of this step arises from the necessity to avoid the interaction between free protein and antibodies that will translate in lower efficiency of the homogeneous immunoassay. Three steps of centrifugation were proposed for both Protein E-AuNPs and BSA-AuNPs.

AuNPs incubated with 0.5 mg/mL of BSA dispersed in acetate buffer were initially centrifuged at 1125×*g* for 30 min. The supernatant was carefully removed and the red pellet was re-suspended pipetting in 1 ml of acetate buffer. A second centrifugation at the same conditions was performed, resulting in a black pellet that could not be re-suspended. To solve this problem, 0.25% of Tween 20 was added to the buffer and the suspension of the BSA-AuNPs was achieved (Figure S2).

To avoid the precipitation the time of centrifugation of the second step was decreased from 30 min to 15 min and the third centrifugation time was also reduced from 15 min to 10 min. The decrease in the centrifugation time enabled the re-suspension of the AuNPs. The buffer used to re-suspend after the third centrifugation step was phosphate buffer saline (PBS). These conditions were also tested and confirmed as optimal with AuNPs conjugated with a solution of 7 mg/ml of BSA. After all centrifugation steps, the supernatant was collected and the UV-Vis spectrum of the supernatant was measured to monitor the amount of BSA present by the presence of a 234 nm peak. In the last step of centrifugation, the amount of BSA in the supernatant was minimum (Figure S3).

In the case of protein E, after the third centrifugation step, the AuNPs exhibited aggregation immediately after the addition of PBS. This is attributed to the presence of sodium chloride. To overcome this, a blocking agent was added to be conjugated to the surface area of the AuNPs which was not conjugated with the target protein. For this system, 500 µl of a solution of BSA 0.2 mg/ml in DI H_2O were used as blocking agent. After rocking for 5 min on ice, 500 µl of PBS were added, and the Protein E- AuNPs show colloidaly stability for a period of 2 hours.

3.4. Anti-BSA antibody detection assays measuring light scattering and light extinction

To determine the sensitivity of the BSA-AuNPs and the optimal conditions to detect anti-BSA antibody, different concentrations of anti-BSA antibody (0.01-10 µg/ml) with different concentrations of BSA (10, 5, 1 µg/ml, 5 µg/ml/0.25% Tween 20 and 5 µg/ml/0.5 M NaCl) were tested using an enzyme linked immunosorbent assay (ELISA). Figure 2 shows that optimal antibody-antigen interaction was

Preprints (www.preprints.org) | NOT PEER-REVIEWED | Posted: 21 August 2018 doi:10.20944/preprints201808.0370.v1

obtained using a 5 µg/ml solution of BSA in the presence of 5 M sodium chloride. In addition, using 1 µg/ml of BSA coating is induced a measurable interaction with respect to the negative control. This suggests that at higher concentrations of BSA, there are other interactions interfering with the detection of the antibody (i.e. double layer of protein). Moreover, it is observed that the presence of Tween 20 in the BSA solution did not have an effect in the interaction between the antibody and the antigen respect to the negative control and other concentrations of BSA coating did not show any significant difference with respect to the negative control. The range of detection of antibody for the BSA solution with NaCl is between 1-5 µg/ml of anti-BSA antibody.

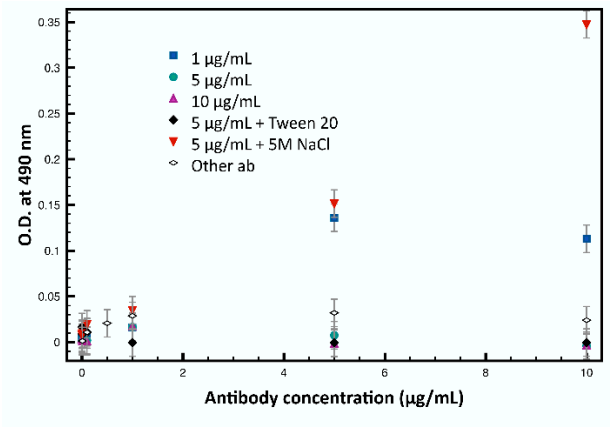

Figure 2. Antibody detection under different coating conditions using ELISA. Microplate results of ELISA with different coating concentrations of BSA (1, 5 and 10 µg/mL) with electrolyte or detergent (Tween 20) addition, testing for detection of a range of antibody anti-BSA concentrations (0-10 µg/mL). Anti-GP1 antibody was used as a negative control.

To evaluate the detection of anti-BSA antibodies by the BSA-AuNPs, based on the results obtained with the ELISA, 100 µl of 5 M NaCl were added to the BSA-AuNPs previous to the addition of the antibody. Static light scattering and visible light extinction of each sample were measured immediately after the addition of the antibody and after 30 min, to monitor changes on the surface of the BSA-AuNPs, presumably caused by the antibody-antigen interaction. Figure 3A shows how visible light extinction spectrum at the plasmon peak increases with the increasing addition of antibody (0.01-0.5 µg/ml). As the quantity of antibody species increases, the light extinction decreases (1-10 µg/ml). This tendency was also reflected in static light scattering (SLS) measurements (Figure 3B).

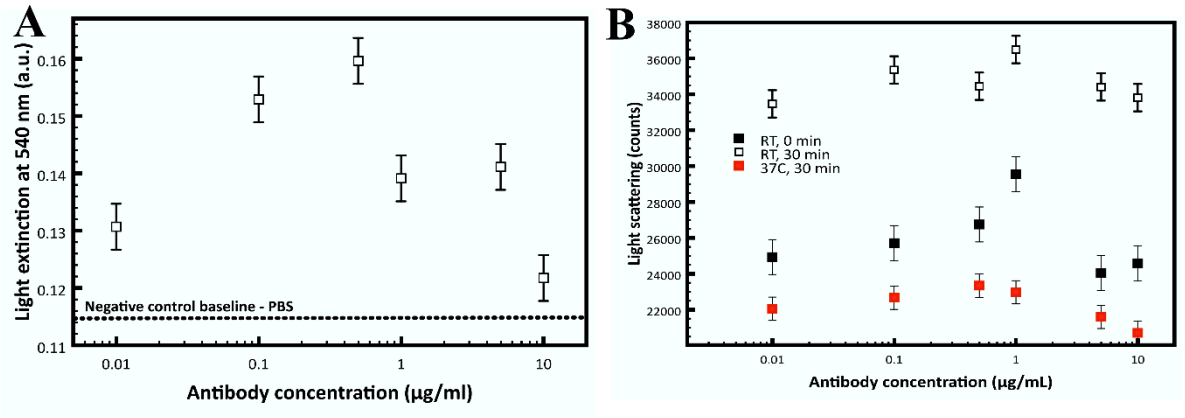

Figure 3. Incubation of antibody with conjugated gold nanoparticles at different temperatures. (**a**) Light extinction at the plasmon peak (540 nm) at RT after 0 min of addition of different concentrations of antibody (0-10 µg/ml) and (**b**) Light scattering at 532 nm measured at RT or at 37 °C after 30 min of addition of 0-10 µg/ml of antibody anti-BSA.

Preprints (www.preprints.org) | NOT PEER-REVIEWED | Posted: 21 August 2018 doi:10.20944/preprints201808.0370.v1

The effect of the temperature on the detection of binding was evaluated. Figure 3B shows static light scattering measurements at room temperature and 37ºC with increasing concentrations of antibody. The tendency of the results is similar at both incubation temperatures whereas the difference in the intensity counts is attributed to the presence of fewer aggregates in solution because the aggregates precipitated over time (30 min).

3.5. Dynamic light scattering for insights into anti-BSA assays

The antibody-antigen interaction using the BSA-AuNPs assay was confirmed by dynamic light scattering (DLS). DLS of gold nanoparticles from the manufacturer suggests a nominal diameter of 65 nm (Figure 4), but the intensity distribution [16] appears to be relatively broad with a significant tail towards larger sizes. In contrast, BSA conjugation appears to significantly narrow the distribution and increase the mean diameter to approximately 80 nm (Figure 4). The intensity distribution change of about 15 nm in diameter appears to be with expected values [16-18] and the stabilization and uniformity generated by the process of protein coating and centrifugation with a surfactant is expected.

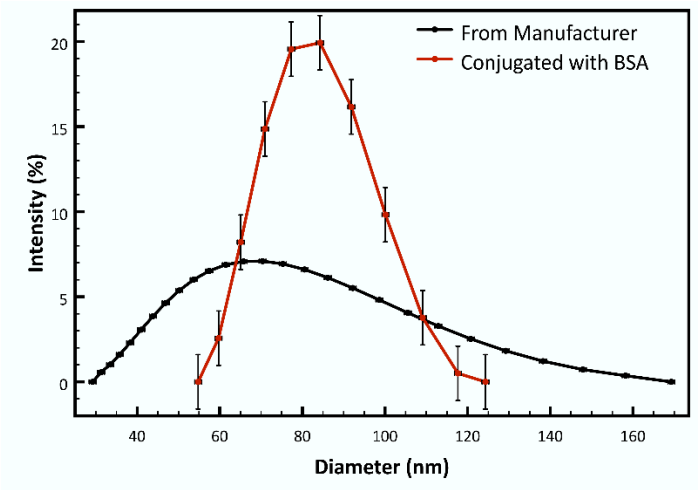

Figure 4. Particle size of conjugated and unconjugated gold nanoparticles. Dynamic Light Scattering intensity distribution measurement of 60 nm gold nanoparticles as is from the manufacturer and after processing to create a coating of BSA.

Size measurements were carried out by DLS on samples of BSA-AuNPs exposed to varying concentration of anti-BSA antibodies from 0-10 µg/ml. These analyses can yield reports of relatively large aggregates even with no addition of antibody and were confirmed by the extinction and SLS results. Leaving the gold nanoparticles in the presence of the antibody overnight at 4 ˚C suggests that it can reverse aggregation by a steric barrier formed by the antibody. Interestingly, when the hydrodynamic radius of different gold nanoparticle sizes is plotted by its intensity distribution, it shifts to higher sizes and the distribution broadens when the particles are interacting with higher concentrations of anti-BSA antibody (Figure 5A). The sole result that does not confirm to the trend seen in Figure 5 is for a sample of 5 microgram per ml of anti-BSA antibody. The experiment was replicated four times, and the cumulants analysis results and average sizes obtained by the intensity distribution, were compared to show the reproducibility of the analyses (Figure 5B). The cumulants analysis results show more consistency with the tendency observed with SLS and UV-Vis spectroscopy, than the results observed with the average size peak.

Preprints (www.preprints.org) | NOT PEER-REVIEWED | Posted: 21 August 2018 doi:10.20944/preprints201808.0370.v1

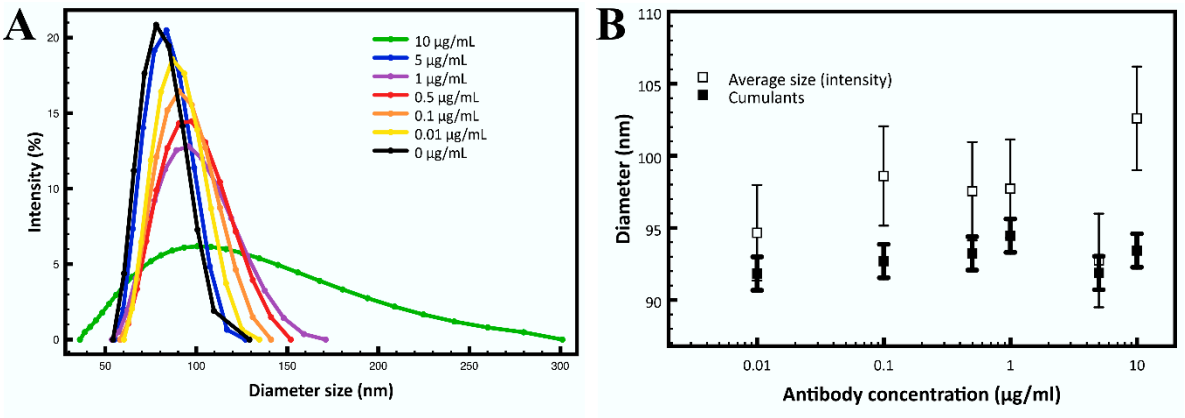

Figure 5. Particle size of conjugated gold nanoparticles in presence of antibody. (**a**) Graph of highest intensity distributions from dynamic light scattering results for anti-BSA assays with antibody concentrations ranging from 0 – 10 micrograms per ml. (**b**) Diameter size obtained with cumulants analysis and average size from intensity distribution when added varying antibody concentrations. Error bars correspond to standard deviation.

3.6. Anti-Protein E antibody detection assays

The detection of Anti-Protein E antibody was evaluated by SLS measurements. Protein E - AuNPs were mixed with different concentrations of antibody anti-protein E (0.01-10 µg/ml). Figure 6 shows that, overall, more light is scattered in the presence of increasing amount of antibody, which indicate interaction of the antibody with the Protein E-AuNPs, except for the average measurement in the presence of 1 µg/ml antibody, which decreased the intensity with respect to the average measurement in the presence of 0.5 µg/ml antibody.

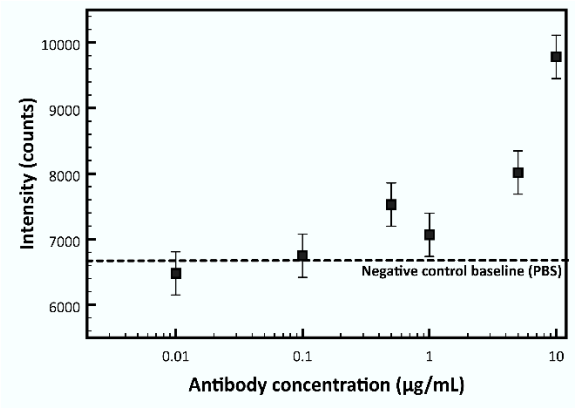

Figure 6. Antibody detection in vitro using light scattering intensity counts. Light scattered of Green light LED at 532 nm by protein E conjugated gold nanoparticles in the presence of different concentrations of antibody anti-protein E (0-10 µg/ml).

The utility of conjugated nanoparticles is most likely in analysis of serum samples from patients, which would have more components such as other antibodies or complement proteins, and may affect results differently than the system tested in vitro. To determine the effect of serum components in SLS and visible light extinction, lyophilized human serum was reconstituted and spiked with a known concentration of antibody was added to protein E-AuNPs. Visible Light extinction spectra and static light scattering were measured for samples spiked with different antibody concentrations and a reconstituted serum sample without antibody, as a negative control. Figure 7 shows that there is a considerable difference in both light extinction (Figure 7A) and light scattered (Figure 7B) by the protein E-AuNPs in the presence of antibody at concentrations equal to or higher than 0.5 µg/ml. This

Preprints (www.preprints.org) | NOT PEER-REVIEWED | Posted: 21 August 2018 doi:10.20944/preprints201808.0370.v1

observation shows that the protein E-AuNPs can effectively detect levels of anti-protein E antibody specifically, despite the presence of other components of human serum, and the method can detect concentrations lower than the minimum levels of IgG or IgM found in human serum (~200 μg/ml) [19].

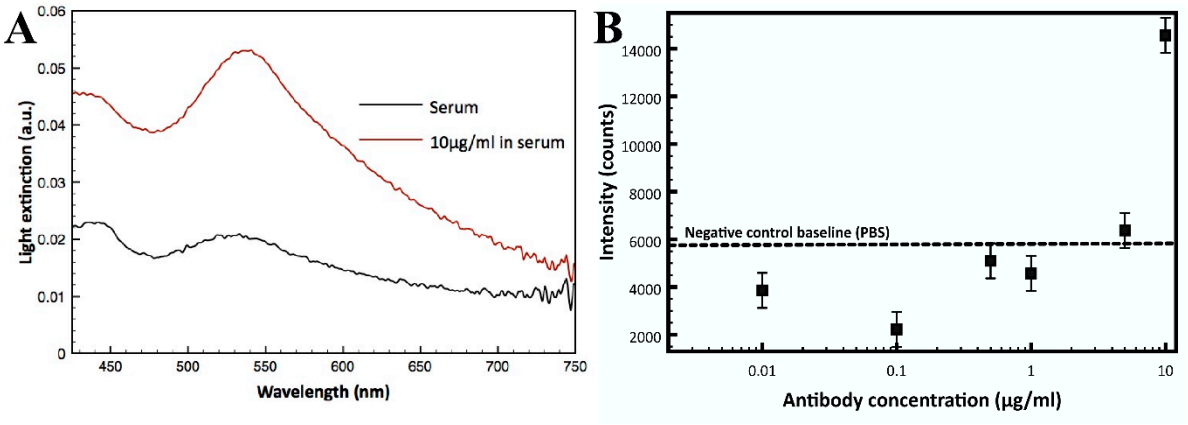

Figure 7. Antibody detection in reconstituted human serum using conjugated gold nanoparticles. (**a**) Light extinction of Protein E conjugated gold nanoparticles in the presence of 10 μg/ml of antibody anti-protein E in human serum, and (**b**) Light scattering of Protein E conjugated gold nanoparticles in the presence 0-10 μg/ml of antibody anti-protein E diluted in human serum. Negative control was human serum with PBS.

4. Discussion

4.1 Binding protein in the immunoassay

The conventional approach to using AuNPs for assays is to perform a titration by continually adding higher concentrations or amounts of protein so that when the mixture is "challenged" by the addition of a high concentration of sodium chloride solution, the amount of protein added that can avoid having the particles aggregate in large numbers to form a purple suspension and subsequent precipitation from solution. This titration test is reasonably simple to conduct and can be a cost-effective way of conjugating AuNPs with expensive proteins or monoclonal antibodies. It also would appear reasonable that adding another protein or blocking agent to cover the surface of AuNPs that may still be exposed leading to unintended non-specific binding, is a complementary step that mirrors traditional ELISA methods. However, this may lead to quite low surface coverage by the protein – as low as 10% [2,10]. Assay sensitivity and analysis speed may be lower as a result since both are driven by the overall antibody accessible protein concentration. Moreover, for the detection of antibodies in response to a disease state, higher surface coverage can improve the probability of bridging multiple particles, given that the target is a polyclonal population of antibodies with multiple binding sites. Therefore, it is recommended that, when possible, the concentration of the protein used for conjugation would be in excess to ensure maximum coverage. However, the practical trade-off between cost and sensitivity/speed is also complicated by the possibility of the blocking agent getting unspecific binding. It may also be useful to determine if BSA, or any other blocking agent used for other protein immunoassays, yields unwanted false positives and if sample components or buffers promote protein-protein aggregation.

4.2. Centrifugation step in the preparation of the immunoassay

Introducing a multi-step centrifugation to remove unbound protein appears to be worthwhile for homogeneous assays based on our experience and reports by several researchers [1,6,9,11,20]. In some published preparations of conjugated of AuNPs, there are membrane or dialysis alternatives to centrifugation [21] but most proteins are too large for proper removal using this method. Moreover, when the technique for supernatant removal is well honed, centrifugation can be done relatively

 doi:10.20944/preprints201808.0370.v1

easily and quickly. We have found that the addition of Tween 20 followed by centrifugation at 4 °C and immediate resuspension (2-3 min) are very important factors for avoiding irreversible aggregation, thus, preventing the loss of AuNPs (Figure S2). Also, time and centrifugation force recommendations published in articles and on commercial web sites should only be regarded as initial guidelines. Shorter times and lower centrifugal speed may provide better and more consistent results. This may be due to the variability of protein coverage and aggregation behaviour for different protein binding preparations. Whatever combination of conditions used, it should be noted that the most important goal of this step is to remove as much unbound protein as possible without significant loss of AuNPs in the suspension or due to pellets that cannot be fully re-suspended.

4.3. Antibody detection and aggregation

One of the more interesting results from our experiments and analyses was in understanding AuNP surface changes in the homogeneous immunoassays by comparing visible extinction, static light scattering, and dynamic light scattering data. The results obtained with the Online Mie Scattering Calculator were a valuable guide in selecting conditions and predicting results [22]. Specifically, the calculator was helpful in selecting the appropriate AuNPs particle size and providing a better understanding of the visible extinction data for the immunoassay measurements since the changes can be subtler near the plasmon resonance peak. In contrast to the research literature [4,9,17,23], which generally provides only one detection method per article, this study goes beyond and compares experimental information with theoretical results that are readily accessible to the reader.

On the other hand, the interpretation of the extinction data can be difficult depending on the calculations carried out to the raw data. While spectra normalization [24] and calculating the ratio of 2 wavelengths for extinction or scattering results [18] have been used and can lead to a useful way of calibrating instruments, these methods also obscure how the entire raw spectra can provide important clues on aggregation before, during or after homogeneous immunoassays are conducted. As seen in Figure 1, there are changes in extinction at wavelengths below the plasmon peak for particles of different diameters. Immunoassay conditions that lead to a small number of low numbers of particles aggregating will increase the light extinction near 400 nm as well as increase the tail of the spectrum at wavelengths greater than the plasmon resonance peak. While impractical for calibration and routine use of immunoassays for detection, fitting predicted extinction curves based on possible aggregate populations to the extinction spectra raw data would nonetheless provide a more mechanistic interpretation of experimental and analytical results.

Another useful illustration of the theoretical calculations is in tracking changes from unmodified AuNPs through aggregate populations in immunoassays. Using the Mie Theory calculator, it can be clearly seen that a layer or corona of protein with a refractive index greater than water (> 1.33 [8]) will increase overall extinction of light and extinction due to scattering. However, at times the extinction and scattering decrease. As noted in Figure 4 with DLS, AuNP aggregation can be dispersed by the addition of protein. Also, unless there is an excessive coating of antibody very much higher than the original protein layer, the expected extinction for AuNP sizes of 60 nm predicted by the calculator should not increase substantially. This is a useful guide to help discern small changes in static light scattering or extinction due to antibody binding versus much larger changes in the spectra or static light scattering when aggregates are formed due to antibody bridging across multiple AuNP with surface protein.

This behavior was also observed in the BSA-AuNPs experiments. In Figure 3, both visible light extinction and light scattering increased the signal progressively, which would indicate aggregation because of antibody bridging. As the antibody concentration increases, it is more probable that two gold nanoparticles are not interacting with the same antibody, but that each nanoparticle has interaction with one or more antibodies separately from other nanoparticles, observed in less aggregation in solution. This tendency was not observed with the detection of anti-protein E antibody

 doi:10.20944/preprints201808.0370.v1

suggesting that the amount of protein E on the AuNP was not covering completely the surface, therefore the need for a blocking agent.

Of particular value is to detect whether the final colloidal solution of conjugated AuNPs is aggregated based on the size versus scattering prediction given in Figure 1. We found that the reference values of no antibody present may be difficult to establish experimentally unless guided by the predicted results. Addition of buffer components to minimize protein-protein aggregation or allowing the prepared AuNPs to be stored overnight and removal of any precipitate can help establish a true "zero" since even a small population of aggregates can increase the scattering significantly. Usually, once antibody is present in solution, those aggregates can tend to dissipate thus lowering the measured scattering and creating a problem in data interpretation, which was observed in Figure 3 after 30 min at 37 ˚C where the tendency was the same, but the intensity decreased. On the contrary, the intensity of the results obtained at room temperature for 30 min was higher than the intensity at other conditions, suggesting the presence of more aggregates due to slower interactions than at higher temperature. Testing the conjugated gold nanoparticles before addition of antibody for light scattering, so that an expected value is achieved, would be a useful step to help obtain more reproducible homogeneous assay results.

DLS results also demonstrated utility in corroborating aggregation and distributions in AuNPs, but there are some challenges in interpreting the information. Khlebstov and Khlebstov [16] points out that there are anomalies when applying DLS to AuNPs. They suggest using intensity distribution rather than number or volume distributions, and our much more limited experience with 60 nm gold particles is an agreement with that recommendation. As shown in the results section, Figure 5 shows a distinct trend in the distribution with higher antibody concentrations for the anti-BSA antibody assay. The overall trend of a broader distribution with a peak maximum shift to higher diameters for higher concentration of anti-BSA antibody resembles the trend in weight distribution of polymers for polymerizations that follow a Schultz-Flory WCLD [25] (Figure S4). The probability of increasing hydrodynamic radius from DLS measurements with higher antibody concentrations suggests that the particle populations follow an increasing probability for longer chains and higher dispersity. However, as noted in the results section, the data in Figure 5 for 5 μg/ml antibody does not follow the trend for this particular sample due to what appears to be large cluster formed rather than a broad distribution. The results are observed with the cumulants analysis were more consistent with the tendency observed with other techniques, and precise than the average diameter size results (Figure 5B). It seems reasonable to assume that both highly distributed and a few highly aggregated populations are possible states given the relatively high concentration of antibody as compared to the number of conjugated AuNPs in the assay.

Lastly, the presence of electrolytes in solution can improve the antigen-antibody interactions, increasing the signal in static light scattering. In the case of the BSA-AuNPs system, we hypothesize that electrolytes help BSA get in a conformation that might be more suitable for the antibody recognition. Nevertheless, the addition of electrolytes is not always necessary. Yeo *et al*. [26] in their study with protein E did not use the addition of electrolytes and had successful results, which confirm the results obtained in this study.

5. Conclusions

The preparation of conjugated AuNPs requires different steps that are crucial for sensitivity, specificity of detection and stability of the conjugated AuNPs. Herein, we optimized the different steps for preparation of conjugated AuNPs. We showed how different amount of protein used for the conjugation step can affect in the antibody detection step and stability, as observed with the results obtained with BSA-AuNPs and Protein E-AuNPs. The amount of protein added depends on several factors, including relative cost and quantity of protein available for assay use. A higher concentration of protein is preferred because it leads to higher gold nanoparticle surface coverage, which would suggest good capacity for immunoassay detection. Centrifugation of the conjugated AuNPs is also key to avoid unspecific binding and therefore skewed results in the antibody detection step.

Another aspect that needs attention is incubation with the target protein (antibody in serum) can be performed at 37 °C to increase the interactions and obtain better assay results. Finally, the addition of electrolytes improved sensitivity measuring intensity counts of light scattering in one of the systems tested. However, the addition of electrolytes is not necessary in every system and the concentration of electrolyte at which it would improve results, needs to be tested in each case.

This study developed a homogeneous immunoassay using AuNPs and optimized the conditions for the preparation of effective conjugated AuNPs to detect antibodies in viral infections. The study can provide a platform for researchers to develop homogeneous immunoassays for rapid detection.

Supplementary Materials: The Supplementary Materials are available online.

Author Contributions: Conceptualization, Antonio A. García; Data curation, Lina S. Franco; Formal analysis, Lina S. Franco, Vladimiro Mujica and Antonio A. García; Investigation, Lina S. Franco and Antonio A. García; Methodology, Lina S. Franco, Vladimiro Mujica and Antonio A. García; Supervision, Vladimiro Mujica, Joseph N. Blattman and Antonio A. García; Validation, Lina S. Franco, Vladimiro Mujica, Joseph N. Blattman and Antonio A. García; Writing – original draft, Lina S. Franco and Antonio A. García; Writing – review & editing, Lina S. Franco and Joseph N. Blattman.

Funding: This research received no external funding.

Acknowledgments: We appreciate the help that Shubhangi Agarwal and Dr. Vikram Kodibagkar provided with running samples and collecting reports using the Dynamic Light Scattering instrument. We thank Dr. Diana Rodriguez for comments that greatly improved the manuscript.

Conflicts of Interest: The authors declare no conflict of interest.

References

1. Huang, S.-H. Gold nanoparticle-based immunochromatographic test for identification of *staphylococcus aureus* from clinical specimens. *Clinica Chim. Acta* **2006**, *373*, 139-143.
2. Engleienne, P. Use of colloidal gold surface plasmon resonance peak shift to infer affinity constants from the interactions between protein antigens and antibodies specific for single or multiple epitopes. *Analyst* **1998**, *123*, 1599-1603.
3. Huang, X.; Jain, P.; El-Sayed, M. Gold nanoparticles: Interesting optical properties and recentapplications in cancer diagnostics and therapy. *Nanomedicine* **2007**, *2*, 681-693.
4. Driskell, J.D.; Jones, C.A.; Tompkins, M.; Tripp, R.A. One-step assay for detecting influenza virus using dynamic light scattering and gold nanoparticles. *Analyst* **2011**, *136*, 3083-3090.
5. Linares, E.M.; Kubota, L.T.; Michaelis, J.; Thalhammer, S. Enhancement of the detection limit for lateral flow immunoassays: Evaluation and comparison of bioconjugates. *J. Immunol Methods* **2012**, *375*, 264-270.
6. Du, B.; Li, Z.; Cheng, Y. Homogeneous immunoassay based on aggregation of antibody-functionalized gold nanoparticles coupled with light scattering detection. *Talanta* **2008**, *75*, 959-964.
7. Kumar, S.; Aaron, J.; Sokolov, K. Directional conjugation of antibodies to nanoparticles for synthesis of multiplexed optical contrast agents with both delivery and targeting moieties. *Nature Protocols* **2008**, *3*, 314-320.
8. Tsai, D.-H.; DelRio, D.W.; Keene, A.M.; Tyner, K.M.; MacCuspie, R.I.; Cho, T.J.; Zachariah, M.R.; Hackley, V.A. Adsoption and conformation of serum abumin protein on gold nanoparticles investigated using dimensional measurements and in situ spectroscopic methods. *Langmuir* **2011**, *27*, 2464-2477.
9. Vidyia, R.; Sreenivasan, K. Selective detection and stimation of c-reactive protein in serum using surface-functionalized gold nano-particles. *Anal. Chim. Acta* **2010**, *662*, 186-192.

10. Brewer, S.; Glomm, W.; Johnson, M.; Knag, M.; Franzen, S. Probing bsa binding to citrate-coated gold nanoparticles and surfaces. *Langmuir* **2005**, *21*, 9303-9307.
11. La Belle, J.T.; Faichild, A.; Demirok, U.K.; Verma, A. Method for fabrication and verification of conjugated nanoparticle-antibody tuning elements for multiplexed electrochemical biosensors. *Methods* **2013**, *61*, 39-51.
12. Sigma-Aldrich, C. Elisa procedures. https://www.sigmaaldrich.com/life-science/cell-biology/antibodies/antibodies-application/protocols/elisa.html
13. Sorensen, C. Q-space analysis of scattering by particles: A review. *J Quant Spectros Radia Transfer* **2013**, *131*, 3-12.
14. Mie, G. Beiträge zur optik trüber medien, speziell kolloidaler metallösungen. *Ann. Phys.* **1908**, *25*, 377-445.
15. Ringe, E.; Sharma, B.; Henry, A.-I.; Marks, L.D.; VanDuyne, R.P. Single nanoparticle plasmonics. *Phys. Chem. Chem. Phys.* **2013**, *15*, 4110-4129.
16. Khlebstov, B.N.; Khlebstov, N.G. On the measurement of gold nanoparticle sizes by the dynamic light scattering method. *Colloid Journal* **2011**, *73*, 118-127.
17. Doak, J.; Gupta, R.; Manivannan, K.; Ghosh, K.; Kahol, P. Effect of particle size distributions on absorbance spectra of gold nanoparticles. *Physica E Low Dimens Syst Nanostruct.* **2010**, *42*, 1605-1609.
18. Haiss, W.; Thanh, N.T.K.; Aveyard, J.; Fernig, D.G. Determination of size and concentration of gold nanoparticles from uv-vis spectra. *Anal. Chem* **2007**, *79*, 4215-4221.
19. Dati, F.; Schumann, G.; Thomas, L.; Aguzzi, F.; Baudner, S.; Bienvenu, J.; Blaabjerg, O.; Blirup-Jensen, S.; Carlstöm, A.; Petersen, P.H., *et al.* Consensus of a group of professional societies and diagnostic companies on guidelines for interim reference ranges for 14 proteins in serum based on the standardization against the ifcc/bcr/cap reference material (crm 470). International federation of clinical chemistry. Community bureau of reference of the commission of the european communities. College of american pathologists. *Eur J Clin Chem Clin Biochem* **1996**, *34*, 517-520.
20. Gilger, C.; Grigiori, F.; De Beaufort, C.; Michel, G.; Freilinger, J.; Hentges, F. Differential binding of igg and iga antibodies to antigenic determinants of bovine serum albumin. *Clin. Exp Immunol* **2001**, *123*, 387-394.
21. Aslan, K.; Holley, P.; Davies, L.; Lakowicz, J.; Geddes, C. Angular-ratiometric plasmon-resonance based light scattering for bioaffinity sensing. *JACS* **2005**, *127*, 12115-12121.
22. NanoComposix. Mie theory calculator. http://nanocomposix.com/pages/tools
23. Thanh, N.; Rosenzweig, Z. Devevelopment of an aggregation-based immunoassay for anti-protein a using gold nanoparticles. *Anal. Chem.* **2002**, *74*, 1624-1628.
24. Amendola, V.; Meneghetti, M. Size evaluation og gold nanoparticles by uv-vis spectroscopy. *J Phys Chem C* **2009**, *113*, 4277-4285.
25. Meira, G.; Oliva, H. Molecular weight distributions in ideal polymerization reactors. An introductory review. *Latin Am. Appl. Res* **2011**, *41*, 389-401.
26. Yeo, E.L.L.; Chua, A.J.S.; Parthasarathy, K.; Yeo, H.Y.; Ng, M.L.; Kah, J.Y.C. Understanding aggregation-based assays: Nature of protein corona and number of epitopes on antigen matters. *RSC Adv* **2015**, *5*, 14982-14993.